Validation of Power Plant Models Using Field Data with Application to the Mostar Hydroelectric Plant

Meaghan Podlaski[a], Xavier Bombois[b], Luigi Vanfretti[a]

[a]*Department of Electrical, Computer, and Systems Engineering, Rensselaer Polytechnic Institute, Troy, NY, USA*
[b]*Laboratoire Ampere, Ecole Centrale de Lyon, Universite de Lyon, Ecully, France*

Abstract

With new technologies being integrated into the existing power system infrastructure and current plants aging, it is increasingly important to maintain accurate dynamic models. A method to individually validate plant component models is proposed, and then is applied to the Mostar hydroelectric power plant using field data obtained during maintenance tests. This methodology is applied for the case where the plant's model is invalid, and then used to re-identify a new model.

Keywords: Power systems modeling, parameter estimation, model validation

1. Nomenclature

AVR	Automatic voltage regulator
dq-axis	Direct-quadrature axis
PSO	Particle swarm optimization
PSS	Power system stabilizer
SMIB	Single machine infinite bus

2. Introduction

2.1. Motivation

Simulation-based studies are indispensable in determining the best practices for power system planning and operation. They give insight on how components will interact dynamically with one another in various operational states. The existing grid infrastructure is aging globally, increasing

the likelihood that plant characteristics have changed over time due to maintenance, electrical overload, and other physical degradation. It is important to ensure that the models representing existing infrastructure, specifically power plants, are valid for performing these studies. Having accurate dynamic models is crucial to understand how planned electrical infrastructure, such as inverter-based resources, e.g. wind and solar generation, interact with the existing system. These inverter-based resources have a significant impact on power system stability characteristics and performance under disturbances, so accurate representation of existing infrastructure is necessary to study the system to the best of our ability for these cases. It is also necessary to maintain accurate models as low confidence in the parameters of individual components in a system leads to more conservative or erroneous assessments and operation.

Highly accurate dynamic power system models are necessary to perform these simulation-based studies. While it is assumed that the plant model is accurate at commissioning time, this situation can change over time. The dynamics of the generator can change due to wear, electrical overload, and maintenance, as replacement of degraded components in the system can result in altered dynamics. The power electronics dynamics present in the AVR have the same behavior and can change over time. Even though it is less likely, the controller parameters of the PSS, AVR and governor can also have been modified without general knowledge, changing their input-output behavior.

This paper presents a methodology based on field data that allows us to verify if the current model of the power system is (likely to be) still valid at any time. The proposed methodology enables us to make this diagnosis independently for each of the power plant components (i.e., the generator, the AVR, the PSS and the governor). In order to do this for an arbitrary component, measurements of the output vector of this component are compared to the output vector predicted by the current model of the component. This predicted output vector is computed by "filtering" the (measured) input vector of a given component by the current model of the component.

The data used in the above mentioned validation procedure can be normal operation data (where the system is basically excited by random load changes). It is to be noted that normal operation data may not be able to detect any dynamics change due to a lack of informativity. Consequently, data obtained during major disturbances could also be used to detect those changes invisible with normal operation data. The system can be excited

with (small) probing tests in order to enhance the detection ability of the proposed validation procedure. A major maintenance could be the ideal moment to gather such informative data (so-called commissioning tests). In particular, the methodology proposed in this paper is here validated based on a set of real measurements obtained during commissioning tests measured at the terminal bus of Mostarsko Blato hydroelectric plant in Bosnia, which produces 30 megawatts [1].

2.2. Related Works

This work builds off of the work in [2] and [3], which focuses on parameter estimation for the Itaipù hydroelectric plant. Itaipù is about 20 times larger than Mostarsko, using phasor measurement unit (PMU) data from various faults and system disturbances. These studies have shown the shortcomings in the user-defined models and the necessity of model maintenance in aging power plants. This study also highlights how plants characteristics change over time.

Most of the previous studies have focused on monitoring the plant online or from disturbance data for the purpose of validation. Ref [4] focuses on the validation and calibration of a 20 MVA hydroelectric plant, which is comparable in size to the Mostarsko plant. The study focuses on testing the plant before, during, and after a generator upgrade project. Six test series were applied to the system, including loss of excitation and load rejection tests. The voltage regulator and machine models calibrated in the study are the most simplified models available, so the parameter estimation is limited.

Ref [5] shows the validation of a power plant using both commissioning tests and fault data. In [5], a fault affects a plant consisting of three thermal generating units. The excitation system/AVR and generator are validated together in these tests; the main benefit of this approach is to be able to validate the model using data collected from actual events that are overlooked in system planning studies. The data is collected at the plant's terminal, so the measurements allow for the plant to be isolated from the rest of the grid; however, the validation method may lead to an erroneous model since all components are lumped together for the validation.

Previous studies for power system model validation using field measurements focus on using disturbance data only. The methods in [6] uses PMU data to determine the cause of faults within the system and calibrate both conventional and renewable plants. The parameter identification uses a combination of particle swarm optimization (PSO) and sensitivity analysis for

a localized portion of the system consisting of a wind turbine and its corresponding reactive power support, step-up and step-down transformers. The calibrated models helped operators find problems with the AVR of the plant for the fault studied, allowing for improved operations under weak grid conditions in the future. This is especially important for a plant like Mostarsko Blato, which provides voltage support and a large local inertia for dynamic stability under fault conditions. As per [7], the location of the Mostarsko plant has significant impact on the local grid's dynamic stability.

Processing monitoring studies have also motivated this work such as [8], which propose methods to monitor the models in closed-loop operation. In this study, a model-based approach is introduced to be exploited for change detection and isolation when the performance of the system degrades. Other process monitoring methods, such as [9], describes how controllers can be altered to optimize system efficiency for controllers developed separately from one another. This is useful for the methodology outlined for the power plant, as it proposes that the components are validated apart from the rest of the system with the goal of re-identifying the components when necessary.

Methods that perform joint estimation of states and parameters have been reported in the literature [10, 11, 12] and have been applied for model validation [13]. However, these methods require continuous excitation to guarantee unbiased estimates. In contrast, our approach can be used when the system is excited or (though with less accuracy) under normal operating conditions.

2.3. Paper Contributions

This paper contributes the following:

- A new methodology for validation of the (current) model of the control system and generator of a power plant using field. The purpose is to determine if these models are still an accurate representation of the elements of the power system. Four elements are validated: the AVR, the PSS, the turbine-governor, and the generator. The methodology is illustrated using data from a hydro-electric power plant obtained during commissioning tests.

- A methodology to update the models when they are no longer an accurate representation of the power system.

2.4. Paper Organization

The paper is organized as follows: the general power plant model and the components are shown in Section III. The proposed validation methodology is described in Section IV. Section V outlines the case study for the Mostar plant, including the introduction of the specific models for the system and data collection method. The validation of the AVR, PSS, and generator using the Mostar data are shown in section VI.

3. Components of the Power Plant

The representative structure of a hydro-electric power plant consists at a minimum of four components: a generator, an automatic voltage regulator (AVR), a power system stabilizer (PSS), and a turbine-governor (TG) as shown in Figure 1. in Figure 1. In this section, we describe these elements in more details with a special attention to their respective inputs and outputs. We suppose that a model of these components is available i.e., a software artifact that allows to compute/predict the output vector of a given components based on the knowledge of its input vector. As mentioned this introduction, we can suppose that these models are accurate at commissioning time; however, the model accuracy can be altered over time. The generator has physical characteristics that can change over time; this can be caused by current overloading on the generator and aging of the plant components. While it is less likely to happen, the controllers have time constants that can be changed in the plants without updating the model accordingly due to human error. The power plant is connected to the electrical grid, which has an influence on the signals that will be measured at the power plant. An appropriate choice of the inputs and outputs of the generator will be necessary to validate the generator models. The electrical power ($P_{elec} + jQ$) measured at the terminal will have to be considered as an input of the generator to effectively separate the grid behavior from the generator.

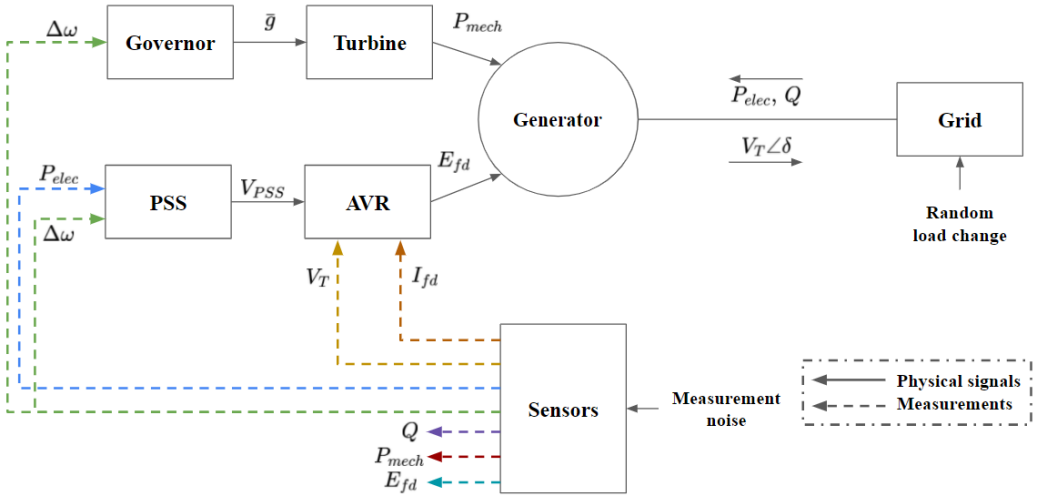

Figure 1: Block diagram of the power plant showing the relationships between each component and their inputs and outputs.

3.1. AVR and exciter model

The automatic voltage regulator, or AVR, is a controller that regulates the voltage of a generator subject to the error between the plant's operating voltage and a reference voltage as well as the field current produced by the generator. It is important to note that, as per common practice, we define the AVR as the combination of a controller and an exciter [14, 15]. The exciter is the power electronics of the excitation system of the power plant that creates the field voltage (E_{fd}) based on the controller portion of the AVR. The controller part of the AVR takes as inputs the control signal (V_{PSS}) generated by the PSS and a measurement ($V_{T,m}$) of the field voltage (V_T). In some configurations, a measurement of the field current (I_{fd}) is also used as an input. As shown in Figure 3, the AVR determines E_{fd} (the output of the AVR) as a function of V_{PSS}, $I_{fd,m}$ and $V_{T,m}$ (the inputs of the AVR). The physical signal E_{fd} is not available, but measurements $E_{fd,m}$ of that physical signal are available. In the AVR, the dynamics of the power electronics are most likely to change over time due to degradation from heat, voltage or current overload, and other stresses on the system.

3.2. PSS model

The power system stabilizer, or PSS, is a controller that adds an additional signal (V_{PSS}) to the AVR with the purpose of controlling the damping of oscillations in the system. The main task of the PSS is to adjust the phase

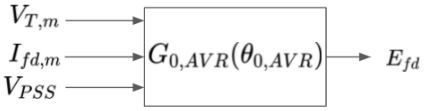

Figure 2: AVR inputs and outputs for static exciter example.

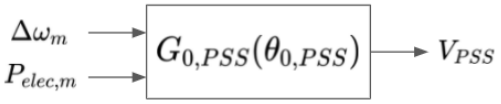

Figure 3: PSS inputs and outputs.

compensation by compensating for phase lags through the generator, excitation system, and power system. The PSS provides torque changes in phase with speed changes to provide damping [15, 16]. The inputs and outputs are further visualized for the PSS in Figure 3. The PSS output is the signal V_{PSS} and the input of the PSS is generally a measurement $\Delta\omega_m$, which is the deviation of the rotational speed of the rotor shaft with respect to its nominal value. In some cases, the PSS has a second input which is a measurement $P_{elec,m}$ of the electrical power. Consequently, the PSS can be seen as an operator that computes V_{PSS} as a function of $\Delta\omega_m$ and $P_{elec,m}$.

3.3. Generator model

As shown in Figure 4, the generator consists of two parts representing the mechanical and electrical behavior in the system. The mechanical part is the physical phenomenon that allows to derive the speed ω of the rotor shaft based on the difference between the mechanical power P_{mech} created by the turbine and the (active) electrical power P_{elec} that is sent to the grid at the terminal voltage. The speed deviation $\Delta\omega$ can then be calculated as the difference between the speed ω and nominal system speed ω_0. This part of the dynamics of the generator is generally described by the swing equation in generator's model. It is to be noted that P_{mech} is created by the turbine using the output $\bar{g}$ of the governor, which is the gate opening of the governor.

The electrical dynamics of the generator are influenced by the field voltage (E_{fd}) and the value of ω. The field current is produced by the electrical portion; the terminal voltage (V_T) is determined based on the complex power ($P_{elec} + jQ$) transmitted to the grid at the terminal voltage. The generator is an operator with inputs P_{mech}, P_{elec}, Q and E_{fd} and outputs ω, V_T and I_{fd}. This means in fact that we can find equations that can compute these outputs based on solely these inputs. It should be noted that the only measurements of P_{elec}, Q, E_{fd}, ω, V_T and I_{fd} are available, the exact values of these quantities are not available. It is to be noted that P_{mech} cannot be measured in practice, but can be computed using a model of the turbine and

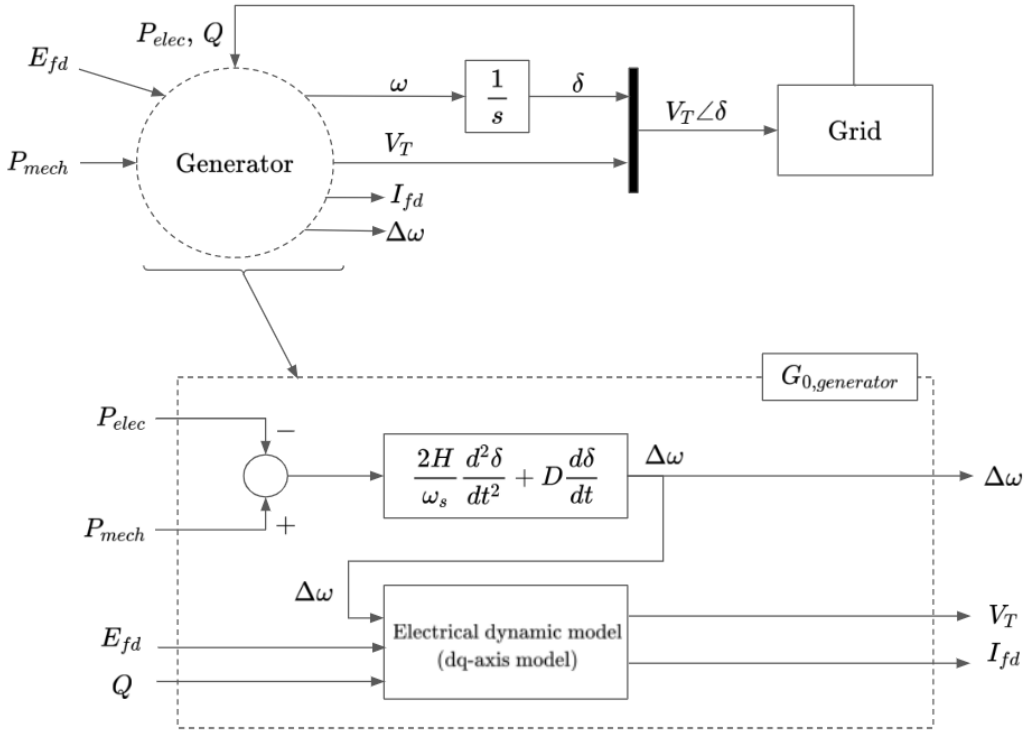

Figure 4: Generator block diagram.

the gate opening $\bar{g}$ (the output of the governor; see next subsection). In this way, we integrate the model of the turbine in the generator model.

3.4. Governor model

The governor is the main controller in a hydraulic turbine system. The governor controls the speed of the generator by varying the water flow through the turbine [17]. Modern turbine control systems include the primary function of the governor, i.e. to maintain and adjust the unit's speed for synchronization with the grid, and have other functions such as to adjust output of the unit in response to operator commands and perform shutdown of the plant.

The inputs and outputs of a hydraulic governor is shown in Figure 5, where the governor system $G_{0,governor}$ is derived in [15]. The definition of each of the parameters are listed in Appendix A. The input of the governor is the deviation from system synchronous speed, $\Delta\omega$. The output of the governor is the gate opening, $\bar{g}$. The governor is a controller that computes

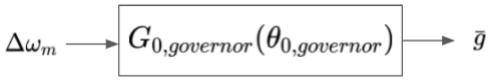

Figure 5: Governor inputs and outputs.

$\bar{g}$ based on $\Delta\omega_m$. It can thus be seen as an operator with as input $\Delta\omega_m$ and with as output $\bar{g}$.

4. Validation Methodology

4.1. Validating Component Models

The system in Figure 1 can be divided into four components to be validated due to the availability of all input/output measurements from the recorded field data: the generator, the AVR, the governor, and the PSS. As described in the previous section, each component of the power plant can be seen as an operator relating inputs and outputs. Let us write these different operators as follows:

$$y_i = G_{0,i} u_i \tag{1}$$

where $i = \{AVR, PSS, generator, governor\}$ and u_i (resp. y_i) is a vector containing the corresponding inputs (resp. outputs). For example, when $i = AVR$, $u_{AVR} = (V_{T,m}, I_{fd,m}, V_{PSS})^T$, $y_{AVR} = E_{fd}$, and $G_{0,AVR}$ represents the dynamical operator relating these inputs and outputs.

At commissioning time, accurate models $M_i (i = \{AVR, PSS, generator, governor\})$ of these different operators $G_{0,i}$ have been determined. We assume that these models M_i were at that time very accurate representations of $G_{0,i}$. Due to the reasons presented in the previous section, the operators $G_{0,i}$ can however change with time and we need to be able to verify whether the models M_i are still good representations of $G_{0,i}$.

When such a validation step is necessary, we collect the input and output vectors u_i and y_i for each component i on the power system (replacing the unknown physical quantities by their measurements when necessary). These data (u_i, y_i) can be collected in normal operations (with the sole excitation of random load changes) or by adding some excitation signals to make the data richer.

Once these data u_i and y_i are collected for all i, we compute the predicted output vector of each model as follows:

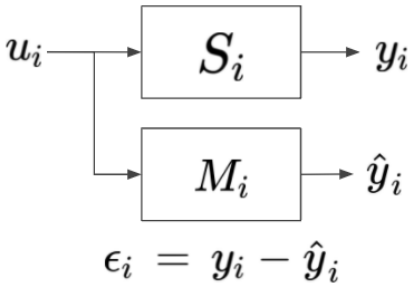

Figure 6: Real system S_i and model M_i comparison.

$$\hat{y}_i = M_i u_i \tag{2}$$

and we verify whether $\hat{y}_i$ is still a good representation of the true output y_i. This can e.g. be done based on the so-called FIT. Let us denote by y_{ij} (resp. $\hat{y}_{ij}$) the j^{th} entry of y_i (resp. $\hat{y}_i$). We define FIT_{ij} as:

$$FIT_{ij} = 100\% \left(1 - \frac{\|y_{ij} - \hat{y}_{ij}\|_2}{\|y_{ij}\|_2}\right) \tag{3}$$

where for any signal $x(t)$, the Euclidean norm $\|x\|_2$ of $x(t)$ is defined as Equation 4.

$$\|x\|_2 = \sqrt{\frac{1}{N}\sum_{t=1}^{N} x^2(t)} \tag{4}$$

For each component i, we thus have n_i FITs where n_i is the dimension of y_i.

The model M_i will be deemed validated if all FIT_{ij} (j=1,...,n_i) yield a value close to the one observed at commissioning. If it is observed for a given component that a FIT_{ij} with a value that has significantly decreased, then the model M_i is no longer a good representation of the dynamic $G_{0,i}$ of component i. In the next section, we show how to update such a model M_i that has become inaccurate.

4.2. Case of invalid models

In the case where the FIT of the component has significantly decreased with respect to the FIT observed at commissioning time, the component model is considered invalid. For each invalid model M_i where $i = \{AVR, PSS,$

$governor, generator\}$, the input/output data (u_i, y_i) will be used to re-identify a new model for that component of the system. Since the components can be validated individually, only the invalid component needs to be re-identified. For this re-identification, the model M_i is parameterized by a number of parameters gathered in a parameter vector θ_i. For each value of θ_i, the model has different dynamics $G_i(\theta_i)$. In particular, the invalidated model M_i was described by $G_i(\theta_{i,init})$ for some value $\theta_{i,init}$ of the parameter vector θ_i.

The new value of the parameter vector will be the one that minimizes the Euclidean norm of $y_i - G_i(\theta_i)u_i$, where (y_i, u_i) is the collected data. The solution of that optimization problem is denoted by $\theta_{i,new}$. This produces a new model $M_{i,new}$ equal to $G_i(\theta_{i,new})$. The quality of this new model can be assessed by computing the FIT corresponding to $M_{i,new}$.

To perform the identification, we will here use RaPId, a MATLAB toolbox for parameter estimation [18]. It should be noted that in [19], the data (u_i, y_i) should be sufficiently rich to ensure the consistency of the re-identified model. This entails in general that the data should have been generated with a sufficient number of excitation signals (see [19]] for more details). Details about computational aspects of RaPId and the algorithms used can be found in [18] and [20], respectively.

Remark. If the re-identified model is still not validated (its FIT is still too low), this could be a sign that the chosen model structure does not correspond to the structure of the true system and should be modified. In other words, the order/complexity of the model should be increased, e.g. in the case of the generator model, instead of using the GENCLS model, we could use a GENSAL model, which is more complex [21].

5. Mostar Power Plant Case Study

5.1. Introduction

In order to validate the proposed approach, the model validation methodology presented previously is applied to the Mostar hydroelectric power plant, using real data to validate the models. The data has been collected after significant maintenance had been performed on the plant, where a large step perturbation V_{step} had been added to the terminal voltage measurement $(V_{T,m})$ with the goal of exciting various functions in the system. The plant consists of the components described in Section III, with the exception of the turbine-governor system for which no measurements were available. Each of the components is validated independently using field data collected during

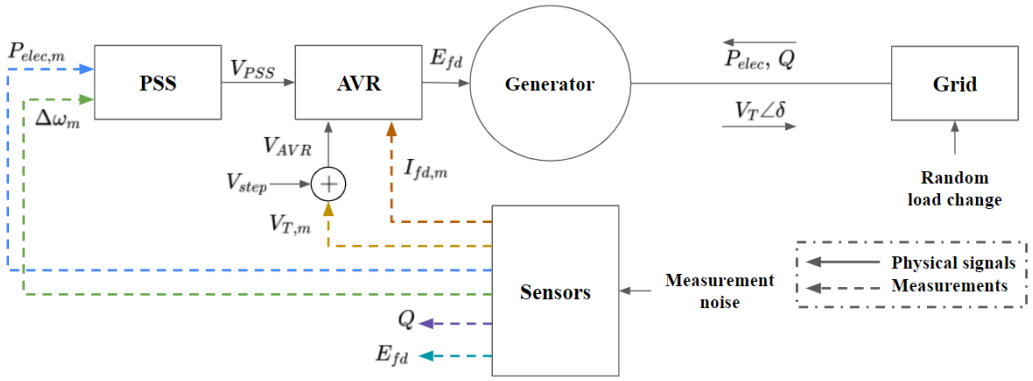

Figure 7: Block diagram of the power plant showing the relationships between each component and their inputs and outputs for the Mostar plant.

commissioning tests, as there is enough data available to validate the components with their inputs and outputs. This specific excitation is depicted in Figure 7 where the first AVR input becomes $V_{AVR} = V_{step} + V_T$.

This excitation V_{step} allows to gather data for the validation of the models M_i of the different components of the Mostar power plant, models that have been provided to us by the engineers at this power plant. These models have all the IEEE standard form [14]. In particular, M_{PSS} is a PSS2B model, with the control block diagram shown in Figure 9. The model M_{AVR} for the AVR is an ST5B model, with the control block diagram in Figure 8. The model $M_{generator}$ of the generator is the salient pole with linear saturation (GENSAL) model with the equations listed in Appendix B. All of the parameters definitions are listed in Appendix A sorted by component type.

Since these commissioning tests focus on testing the functionalities of the electrical controllers, the measurements of the turbine and governor are unavailable. As a result, the models for these components are not included in the model in Figure 7. It is assumed that the mechanical power (P_{mech}) is a constant value that is derived during the initialization of the model as a result of the power flow.

5.2. AVR and excitation system model

The AVR and excitation system is represented by the IEEE ST5B standard model [14, 22], with the complete transfer function model shown in Figure 8. The unit has a static potential-source excitation system, meaning the voltage is transformed to an appropriate level using a controlled-rectifier.

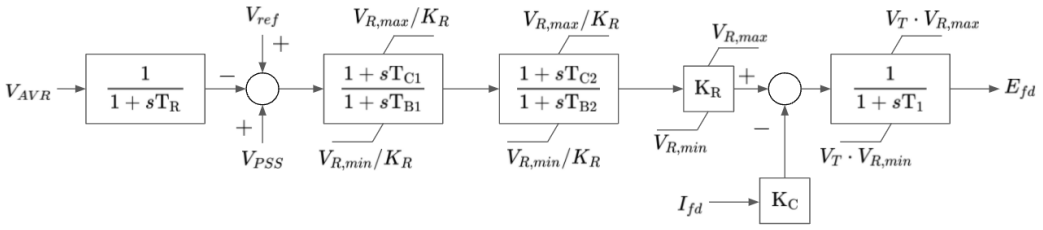

Figure 8: AVR ST5B block diagram.

Controlled-rectifiers provide the necessary direct current for the generator field.

The input AVR voltage is the sum of the machine voltage and step excitation ($V_{AVR} = V_T + V_{step}$), which is passed through a transducer delay lag:

$$\frac{1}{1+sT_R} \tag{5}$$

where the output is used to calculate the error between the reference voltage (V_{ref}) and PSS voltage (V_{PSS}). This transfer function is used to account for the time delay created by the sensors measurements. The reference voltage (V_{ref}) is a pre-defined set point value for the controller, not an input. The definition of each parameter is listed in Appendix A.

In this configuration, we assume a continuous time controller, so the main regulator transfer function consists of two anti-windup lead-lad blocks and a gain:

$$K_R \frac{1+sT_{C1}}{1+sT_{B1}} \frac{1+sT_{C2}}{1+sT_{B2}} \tag{6}$$

The difference between the regulator transfer function and the field current (I_{fd}) scaled by the rectifier regulation factor (K_C) is then applied to the transfer function for the power electronics:

$$\frac{1}{1+sT_1} \tag{7}$$

Since the commissioning tests do not excite the system such that the controller would experience a fast perturbation, the rectifier function has little effect on the system. If the system were subject to a fault, the rectifier function will have an impact on the AVR model response. The most crucial functions in the controller are represented by the main regulator transfer functions.

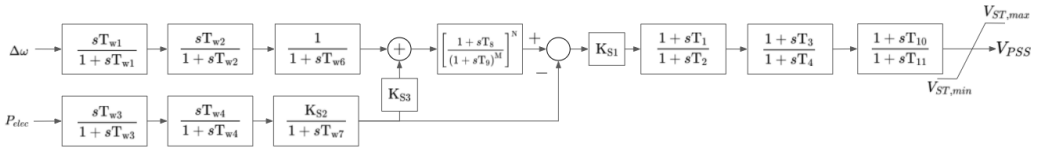

Figure 9: PSS2B block diagram.

5.3. PSS model

The power system stabilizer, or PSS, is a controller that adds an additional signal to the AVR with the purpose of controlling the damping of oscillations in the system. The Mostar plant uses the IEEE PSS2B model to represent the PSS controller [14, 16]. The inputs and outputs of the PSS are shown in Figure 9, where the inputs of the generator speed deviation ($\Delta\omega$) and electric power (P_{elec}). The output of the PSS is the PSS voltage (V_{PSS}), which is subsequently used as an input to the AVR. The description of all of the time constants, gains, and other variables used in the PSS in Figure 9 are listed in Appendix A. The AVR model is compatible with the PSS2B PSS model [14].

The PSS is a dual-input controller that uses the machine speed and electrical power to calculate the integral of the accelerating power to make the calculated stabilizer signal insensitive to mechanical power change. Each input has two washouts ($T_{w1}, T_{w2}, T_{w3}, T_{w4}$) represented as well as transducer time constants (T_6, T_7). To determine the integral of accelerating power of the PSS, the gain K_{S2} would be:

$$K_{S2} = \frac{T_7}{2H} \tag{8}$$

where H is the total shaft inertia of all mechanically connected rotating components of the unit. In the case of Mostar, the unit is represented as one machine, so H is the shaft inertia of the generator. The exponents M and N allow for a "ramp-tracking" characteristic to be represented in the controller; phase compensation is provided by the three lag-lead blocks with time constants $T_1, T_2, T_3, T_4, T_{10}, T_{11}$. The output of the controller is limited by the minimum and maximum setpoints, $V_{ST,min}$ and $V_{ST,max}$.

5.4. Generator model

The Mostar plant uses a salient pole generator with linear saturation, for which all equations are shown in Appendix A [23]. The generator is

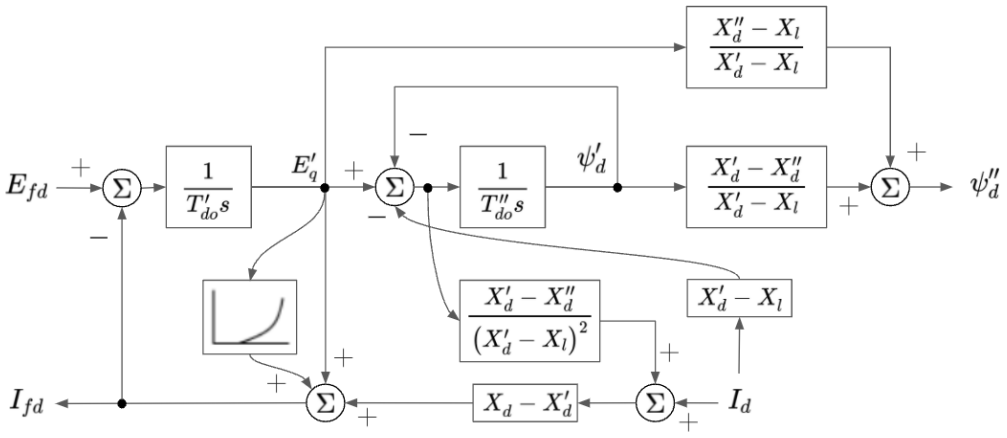

Figure 10: Generator direct axis block diagram.

represented in a direct-quadrature axis equivalent structure. In geometric terms, the d and q axes are per-phase representations of the flux contributed by the three separate sinusoidal phase quantities at the same frequency. The flux produced by the field winding is located on the d-axis; the q-axis is the axis where the torque is produced. The block diagram for the direct axis is shown in Figure 10, where E_{fd} is the field voltage signal produced by the AVR. The model also uses the direct-axis current I_d as an input. The output I_{fd} directly feeds back to the AVR, and Ψ''_d is the sub-transient flux which is further used to calculate the terminal voltage of the machine. The d-axis component of the terminal voltage is shown in Equations 9 and 10. Equation 9 calculates the total flux through the d-axis Ψ_d, where I_d is the current through the d-axis, X''_d is the sub-transient d-axis reactance, and Ψ''_d is the sub-transient flux shown as the output of the generator in Figure 10.

$$\Psi_d = \Psi"_d - X"_d * I_d \tag{9}$$

$$u_d = (-\Psi_q) - R_a * I_d \tag{10}$$

The block diagram of the quadrature axis is shown in Figure 11, where the quadrature current I_q is the input to the system and q-axis sub-transient Ψ''_q flux is the output. These are based on the equations in Appendix A. The q-axis component of the terminal voltage is shown in Equations 9 and 10. Equation 9 calculates the total flux through the q-axis Ψ_q, where I_q is the current through the q-axis, X''_q is the sub-transient d-axis reactance, and Ψ''_q

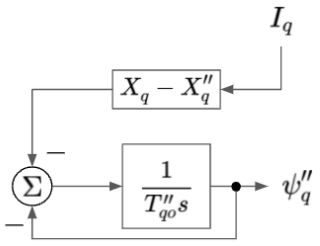

Figure 11: Generator quadrature axis block diagram.

is the sub-transient flux shown as the output of the generator in Figure 11.

$$\Psi_q = \Psi"_q - X"_q * I_q \tag{11}$$

$$u_q = \Psi_d - R_a * I_q \tag{12}$$

6. Mostar Power Plant Validation

Each of the specific models outlined in Section V is validated using the methodology from Section IV. The inputs and outputs of the components are selected based on the relationships shown in the system block diagram in Figure 7 using the data available. The data are collected using a sampling rate of 5ms.

6.1. AVR and excitation system model validation

As explained in Section V, the AVR input vector is $u_{AVR} = [V_{T,m}, V_{PSS}, I_{fd,m}]\top$ and its output $y_{AVR} = E_{fd}$, which will be approximated by $y_{AVR} = E_{fd,m}$. The response of the model is $\hat{y}_{AVR} = M_{AVR}u_{AVR}$, where M_{AVR} has the structure given in Figure 8. In Figure 12a, the different inputs in u_{AVR} are represented while y_{AVR} and $\hat{y}_{AVR}$ are compared in Figure 12b. In this last figure, we observe that $\hat{y}_{AVR}$ is almost equal to the actual output y_{AVR} ($FIT_{AVR} = 96.39\%$). The model M_{AVR} can be thus deemed validated.

6.2. Generator model validation

Let us now consider the next component: the generator. Recall that we do not have turbine governor measurements, so P_{mech} will therefore be assumed constant and computed from the plant's dispatch of P_{elec}. Consequently, the generator input vector is $u_{generator} = (E_{fd}, P_{elec}, Q)$ and its output $y_{gen} = (\Delta\omega, V_T, I_{fd})$. As previously stated, the physical quantities will be replaced by their measurements in $u_{generator}$ and $y_{generator}$.

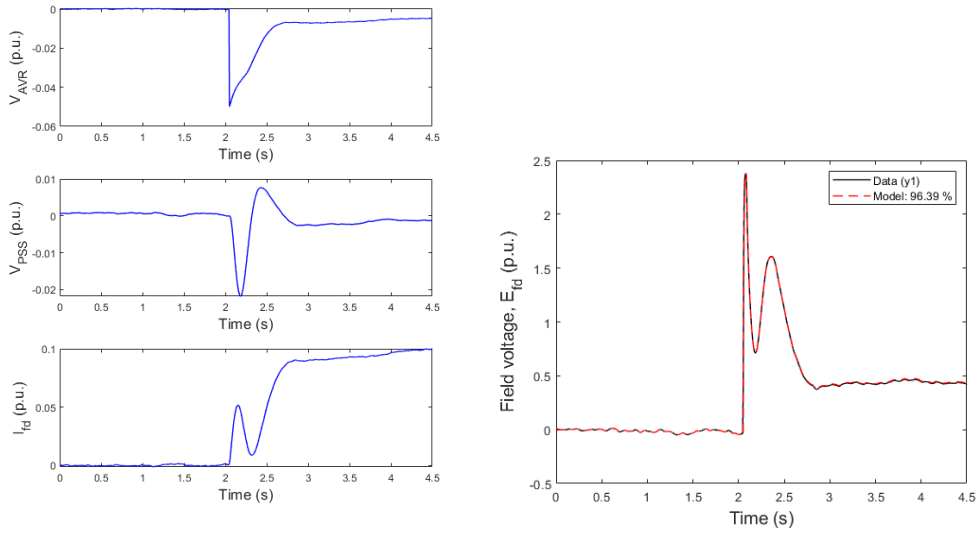

(a) Inputs to AVR. (b) AVR field voltage response comparison.

Figure 12: AVR validation data and results.

The measurement of $\Delta\omega$ was not collected during the commissioning tests, so this output will not be considered in the validation. The output vector therefore reduces to $y_{generator} = (V_T, I_{fd})$.

Using $M_{generator}$, We then compute $\hat{y}_{generator} = M_{generator} u_{generator}$. In Figure 13a, the different inputs in $u_{generator}$ are represented while $y_{generator}$ and $\hat{y}_{generator}$are compared in Figure 13a. In Figure 13b, we here also observe that both entries of $\hat{y}_{generator}$ are almost equal to the entries of the actual output vector $y_{generator}$ ($FIT_{generator} = 99\%$ for both entries). The model $M_{generator}$ can be thus deemed validated.

6.3. PSS model validation

As explained in Section V, the PSS input vector is $u_{PSS} = [\Delta\omega_m, P_{e,m}]^\top$ and its output $y_{PSS} = V_{PSS}$. We compute $\hat{y}_{PSS} = M_{PSS} u_{PSS}$. Since the measurement for ω was not collected from the commissioning test, input data for $\Delta\omega_m$ comes from the simulation of the validated generator model. In Figure 14a, the different inputs in u_{PSS} are represented while y_{PSS} and $\hat{y}_{PSS}$ are compared in Figure 14b. In Figure 14b, we observe that $\hat{y}_{PSS}$ is here also almost equal to the actual output y_{PSS} ($FIT_{PSS} = 97.32\%$). The model M_{PSS} can be thus deemed validated.

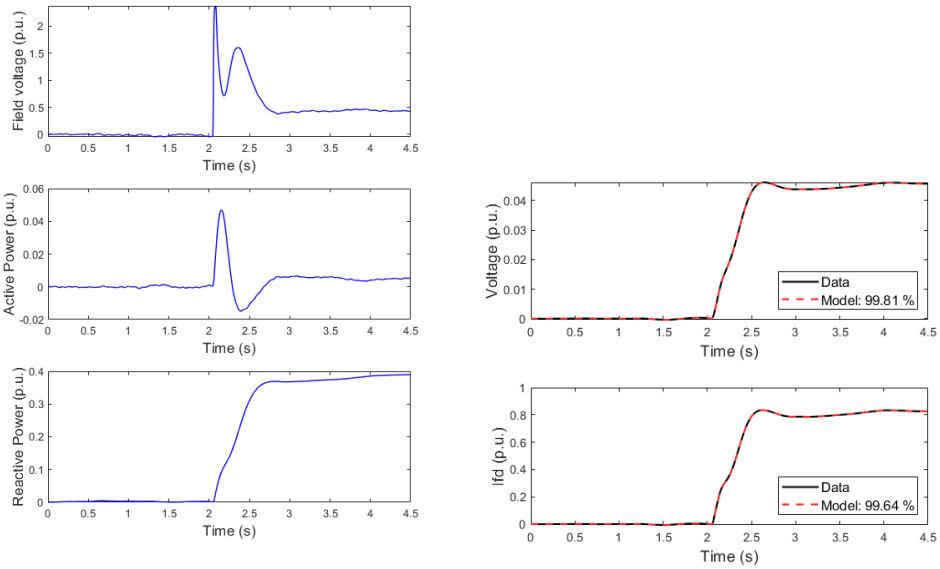

(a) Inputs to generator. (b) Generator output response comparison.

Figure 13: Generator validation inputs and results for correct inputs/outputs to separate grid behavior from generator.

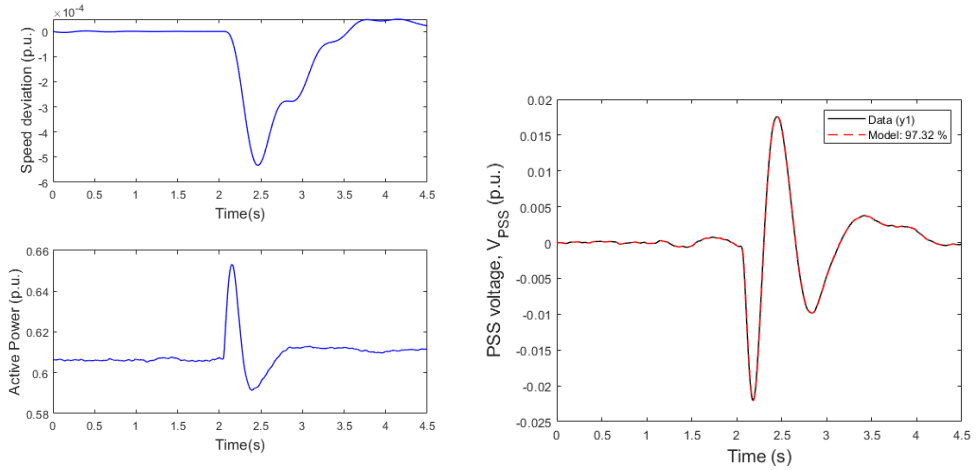

(a) Inputs to PSS. (b) AVR field voltage response comparison.

Figure 14: PSS validation data and results.

7. Validation Based on Simulation Data

Using Mostar's measurement data, the commissioning models M_i remain validated. Now we consider a simulation study to show that the method pre-

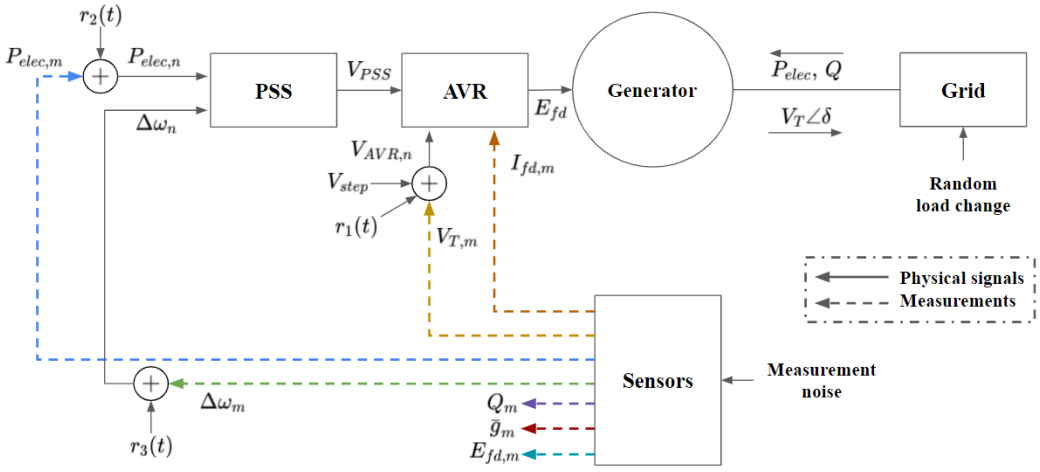

Figure 15: Block diagram of the power plant showing the relationships between each component and their inputs and outputs for the Mostar plant.

sented in Section IV can detect a change on the system's dynamics. In this simulation study, the Mostar power plant (with no governor) is represented by the models M_i of the different components validated in the previous section. Some of the parameters of the original models will be modified in the simulator to show that the original models will not longer be validated by the model validation procedure.

As a first example, we increase the value of the generator parameter X_d by 10%. In the simulator of the power plant, the value of X_d is equal to 1.3013 p.u. while, in $M_{generator}$, $X_d = 1.183$ p.u. We collect data on the simulator of the power system by applying, in addition to the step excitation V_{step}, three (small) white noise excitation signals $r_k \quad (k = 1, 2, 3)$ at different locations (see Figure 15). Using [19], it is clear that these data will be sufficiently rich to re-identify the system if it is necessary.

Since $G_{0,AVR} = M_{AVR}$ and $G_{0,PSS} = M_{PSS}$ in the simulator, we expect that M_{AVR} and M_{PSS} will be deemed validated using the simulation data and that is indeed the case. As far as the generator is concerned, the results are depicted in Figure 16 (representing the input vector $u_{generator}$) and Figure 17a representing $y_{generator}$ and $\hat{y}_{generator} = M_{generator}u_{generator}$ where we observe a significant difference between the predicted terminal voltage and the observed terminal voltage. The generator model $M_{generator}$ is thus invalidated and the identification procedure described in Section IV.A is launched to update the parameters of the model. In Table 1, the identified parameter

vector $\theta_{generator,new}$ is compared to the true value of this parameter vector (the one used in the simulator) and we see that the identification procedure allows to obtain sufficiently close estimates of all parameters. This is confirmed by comparing $y_{generator}$ to $\hat{y}_{generator,new} = M_{generator,new}u_{generator}$ (where $M_{generator,new}$ is the model of the generator with the parameter vector $\theta_{generator,new}$). This comparison is done in Figure 17b where we can see that predicted outputs and actual outputs are very close ($M_{generator,new}$ can thus be deemed validated).

Let us finally consider another case that stresses the importance of rich data for the validation step. We now consider a simulator where $G_{0,generator} = M_{generator}$ and $G_{0,AVR} = M_{AVR}$ and where the washout constants of the PSS (see Figure 9) are modified with respect to M_{PSS}. We consider here the case where these constants are all doubled and the case where they are all halved. If the excitation is only a step added at the measurement of V_T, the model M_{PSS} remains validated even though $G_{0,PSS} \neq M_{PSS}$, as shown in Figure 19a and 19b. This is due to the fact that the step on $V_{T,m}$ does not have a strong influence $\Delta\omega_m$, the signal driving the part of the PSS containing these washout constants.

If we now consider the multiple excitation signals shown in Figure 15 (where the excitation r_2 is added to $\Delta\omega_m$), the validation procedure succeeds in detecting the change in the PSS as shown in Figures 20a and 20b where y_{PSS} is compared with $\hat{y}_{PSS} = M_{PSS}u_{PSS}$ for both halved and doubled time constants respectively.

8. Conclusion and Future Works

In this paper, a methodology for component validation for power plants has been proposed and effectively tested using both real-world and simulation data. The controllers and the generators can be separately validated from each other by having sufficiently informative data for each selected input/output of the system. In the case of invalidated models, a method to re-validate and re-identify the component model is introduced. This methodology is applied using measurements collected from the Mostar hydroelectric plant.

Using test data from the Mostar plant, we can distinguish inputs and outputs to validate each of the three elements in the plant. A good validation of the three elements can be obtained based on the results presented in Sections V to VII. The AVR and PSS have inputs and outputs that can be

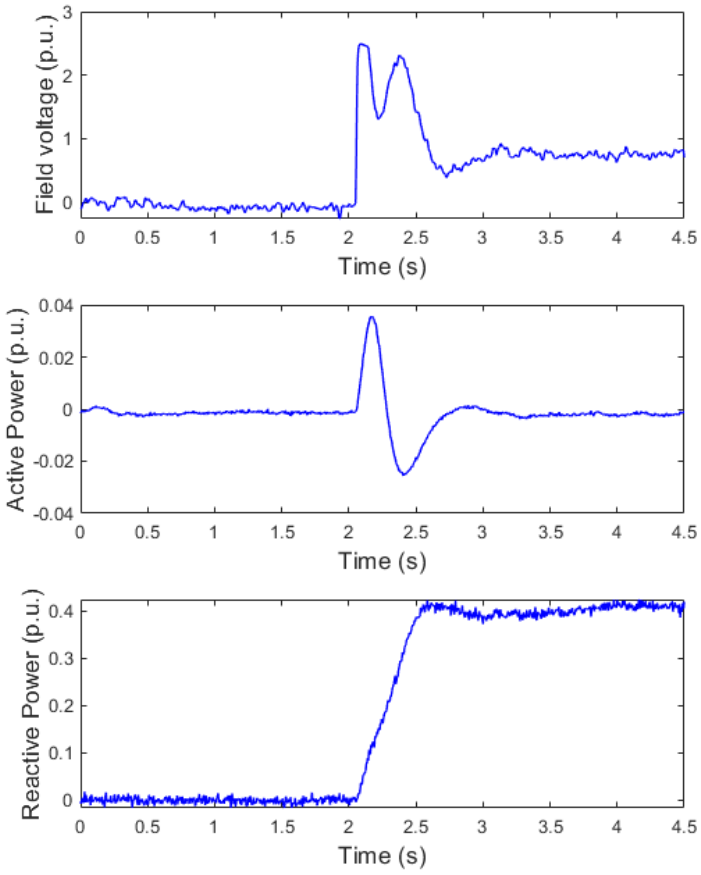

Figure 16: Inputs to generator in case of changed parameters.

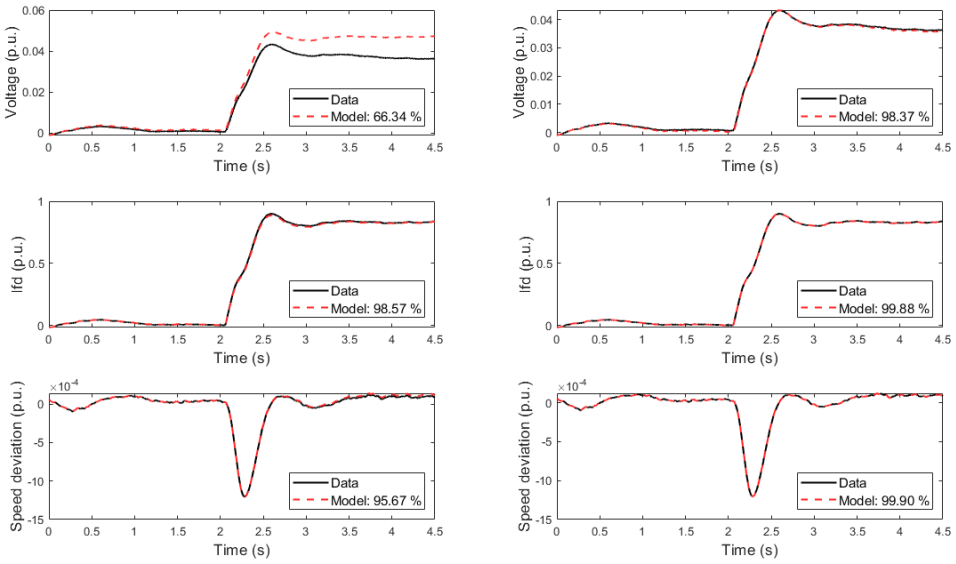

(a) Invalidated generator model response. (b) Validated generator model response with re-identified models.

Figure 17: Generator validation results for when X_d is increased by 10%.

intuitively chosen to validate the model; however, the inputs and outputs of the generator must be selected to separate the generator from the rest of the grid. When the conventional inputs and outputs are chosen to validate the generator, the dynamic behavior is influenced by the grid. By following the equations of the model instead, like shown in Figure 4, the component can be effectively isolated. Once the correct inputs and outputs were selected for each component, they each had a high FIT to the data and are considered valid.

The major concern of these systems is that the properties of the generator can change over time [23]. After re-identifing the model, the parameters of the new model are close to the actual system. Since the components can be separately validated, it is only necessary to re-identify and re-validate the affected component. This is incredibly valuable when re-validating the plant using optimization methods to solve the objective function of the problem, as the optimization problem is focused on fewer parameters. This reduces the chance of the solution of the parameter estimation arriving at a local

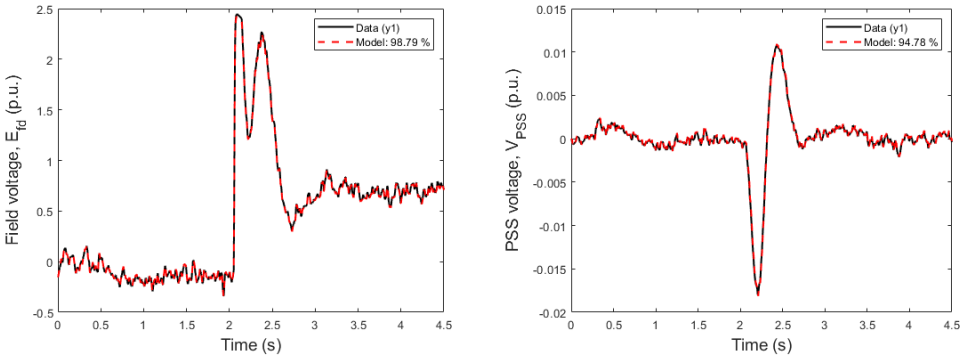

(a) AVR validation. (b) PSS validation.

Figure 18: Controller validation when there is a change in generator parameters.

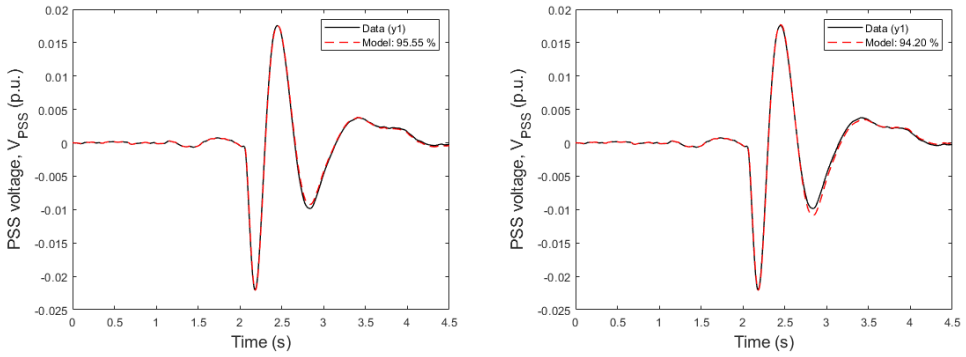

(a) PSS with halved time constants for T_{w1}, T_{w2}, T_6.

(b) PSS with doubled time constants for T_{w1}, T_{w2}, T_6.

Figure 19: PSS informativity issues with $\Delta\omega$ input.

Table 1: Generator parameters for re-identified model due to 10% increase on X_d

	X_d	R_a	H	D
True generator parameters	1.3013	0.004799	2.137	0
Identified generator parameters	1.318	0.00471	2.148	0
Relative error (%)	1.28	1.85	0.51	0
	X'_d	X_q	$X"_d$	$X"_q$
True generator parameters	0.371	0.62	0.215	0.241
Identified generator parameters	0.367	0.63	0.2166	0.239
Relative error (%)	1.08	1.61	0.74	0.83
	X_l	T'_{d0}	$T"_{d0}$	$T"_{q0}$
True generator parameters	0.1	3.77	0.0552	0.0823
Identified generator parameters	0.1001	3.775	0.0601	0.0775
Relative error (%)	0.1	0.13	8.8	5.83

minimum and decreases the time needed to re-identify the model.

Additional cases of the generator parameter changes will be studied in the future when appropriate real-world data is available, analyzing changes to both the excitation system and mechanical system, which will result in changed behavior in the swing equations.

Acknowledgements

The work of M. Podlaski is supported by the National Science Foundation Graduate Research Fellowship Program under Grant No. DGE 1744655 and the Chateaubriand Fellowship of the Office for Science & Technology of the Embassy of France in the United States.

The work of L. Vanfretti was supported in part by Dominion Energy Virginia.

The authors thankfully acknowledge the support of Zdravko Rabuzin of Advensys Engineering Ltd. for providing the data of the hydroelectric power plant.

Declaration of Competing Interest

The authors declare that they have no known competing financial interests or personal relationships that could have appeared to influence the work

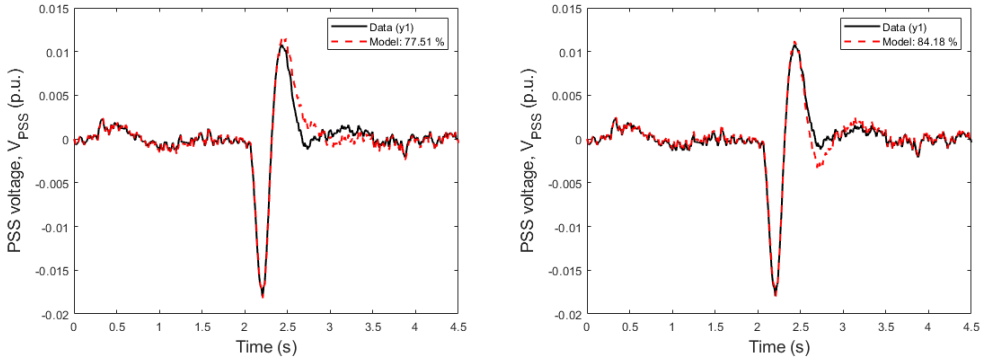

(a) PSS with halved time constants for T_{w1}, T_{w2}, T_6.

(b) PSS with doubled time constants for T_{w1}, T_{w2}, T_6.

Figure 20: PSS informativity issues with $\Delta\omega$ input.

reported in this paper.

CRediT authorship contribution statement

Meaghan Podlaski Conceptualization, methodology, software, validation, visualization, writing - original draft. **Xavier Bombois** Conceptualization, methodology, validation, resources, supervision, writing - review & editing. **Luigi Vanfretti** Conceptualization, software, resources, supervision, writing - review & editing.

Appendix A. Parameter Definitions

Generator - IEEE GENSAL Model	
T'_{d0}	d-axis transient open circuit time constant
T''_{d0}	d-axis sub transient open circuit time constant
T''_{q0}	q-axis sub transient open circuit time constant
H	Inertia constant
D	Speed damping
X_d	d-axis reactance
X'_d	d-axis transient reactance
X''_d	d-axis sub transient reactance
X''_q	q-axis sub transient reactance
X_q	q-axis reactance
X_l	leakage reactance

AVR - IEEE ST5B	
T_r	Filter time constant
T_{C1}	Regulator lead time constant 1
T_{B1}	Regulator lag time constant 1
T_{C2}	Regulator lead time constant 2
T_{B2}	Regulator lag time constant 2
K_R	Regulator gain
K_C	Rectifier regulation factor
T_1	Rectifier time constant

PSS - IEEE PSS2A	
T_{w1}	First washout time on signal 1
T_{w2}	Second washout on signal 1
T_{w3}	First washout on signal 2
T_{w4}	Second washout on signal 2
T_{w6}	Time constant on signal 1
T_{w7}	Time constant on signal 2
T_1	Lead/lag time constant
T_2	Lead/lag time constant
T_3	Lead/lag time constant
T_4	Lead/lag time constant
T_8	Lead of ramp tracking filter
T_9	Lag of ramp tracking filter
T_{10}	Lead/lag time constant
T_{11}	Lead/lag time constant
K_{S1}	PSS gain
K_{S2}	Gain on signal 2
K_{S3}	Gain on signal 2 input
$V_{ST,max}$	PSS output max limit
$V_{ST,min}$	PSS output min limit
$V_{SI1,max}$	Input signal 1 max limit
$V_{SI1,min}$	Input signal 1 min limit
$V_{SI2,max}$	Input signal 2 max limit
$V_{SI2,min}$	Input signal 2 min limit
M	Denominator order of ramp tracking filter
N	Order of ramp tracking filter

Governor	
T_p	Pilot valve and servomotor time constant
K_s	Servo gain
T_G	FMain servo time constant
R_p	Permanent droop
R_T	Temporary droop
T_R	Reset time
$R_{max,open}$	Maximum gate opening rate
$R_{max,close}$	Maximum gate closing rate
$R_{max,buff}$	Maximum gate opening rate in buffered region
g_{buff}	Buffered region in pu of servomotor stroke

Appendix B. IEEE standard model equations

GENSAL generator

$$K_{1d} = \frac{(X'_d - X"_d)(X_d - X'_d)}{(X'_d - X_l)^2}$$

$$K_{2d} = \frac{(X'_d - X_l) * (X"_d - X_l)}{(X'_d - X"_d)}$$

$$K_{3d} = \frac{X"_d - X_l}{X'_d - X_l}$$

$$K_{4d} = \frac{X'_d - X"_d}{X'_d - X_l}$$

$$\frac{dE'_q}{dt} = \frac{1}{T'_{d0}}(E_{fd} - X_{ad} I_{fd})$$

$$\frac{d\Psi_{kd}}{dt} = \frac{1}{T"_{d0}}(E'_q - \Psi_{kd} - (X'_d - X_l) * I_d)$$

$$\frac{d\Psi"_q}{dt} = \frac{1}{T"_{q0}}(-\Psi"_q + (X_q - X"_q) * I_d)$$

$$\Psi_{d"} = E'_q + K_{3d} + \Psi_{kd} K_{4d}$$

$$\Psi_d = \Psi"_d - X"_d * I_d$$

$$\Psi_q = -\Psi"_q - X"_q * I_q$$

$$X_{ad} I_{fd} = K_{1d} * (E'_q - \Psi_{kd} - (X'_d - X_l) * I_d)$$
$$+(X_d - X'_d) * I_d + (SE_{linear} + 1) * E'_q$$

$$T_e = \Psi_d * I_q - \Psi_q * I_d$$

$$u_d = (-\Psi_q) - R_a * I_d$$

$$u_q = \Psi_d - R_a * I_q$$

Generator variables	
K_{1d}	Generator constant 1
K_{2d}	Generator constant 2
K_{3d}	Generator constant 3
K_{4d}	Generator constant 4
E'_q	q-axis voltage behind transient reactance
Ψ_{kd}	d-axis rotor flux linkage
Ψ''_d	d-axis subtransient flux linkage
Ψ''_q	q-axis subtransient flux linkage
Ψ_d	d-axis flux linkage
Ψ_q	q-axis flux linkage
I_d	d-axis armature current (p.u.)
I_q	q-axis armature current (p.u.)
SE_{linear}	linear saturation function
T_e	Electrical torque (p.u.)
u_d	d-axis terminal voltage (p.u.)
u_q	q-axis terminal voltage (p.u.)

Appendix C. Impact of grid on generator validation

The grid can affect the generator response if the incorrect inputs and outputs are chosen for model validation. Using the inputs and outputs in Equation C.1, the generator model is deemed invalid. The incorrect choice for the generator inputs and outputs can be chosen based on the signals shown in Figure 1, where the plant's mechanical power (P_{mech}) and field voltage (E_{fd}) are used as the inputs for validation. The outputs would be the field current (I_{fd}), active/electrical power (P_{elec}), and reactive power (Q). The inputs and outputs of the plant would be:

$$\hat{y}_{gen} = M_{gen} u_{gen} \tag{C.1}$$

$$\begin{bmatrix} P_{elec} \\ Q \\ V_T \end{bmatrix} = M_{gen} \begin{bmatrix} E_{fd} \\ P_{mech} \end{bmatrix} \tag{C.2}$$

The response of the generator in Figure C.21b shows that the voltage and reactive power settle to the wrong operating point after applying the field voltage, giving a fit of 33.07% for active power (P_{elec}), 86.74% for reactive power (Q), and 88.61% for machine terminal voltage (V_T). Evidently, the generator and grid are lumped into the same model by selecting these inputs and outputs, which results in an invalid generator model.

By selecting the field voltage as the only input, the active and reactive power produced by the generator are also affected by some of the grid dynamic behavior. This means the generator model isn't isolated in our analysis.

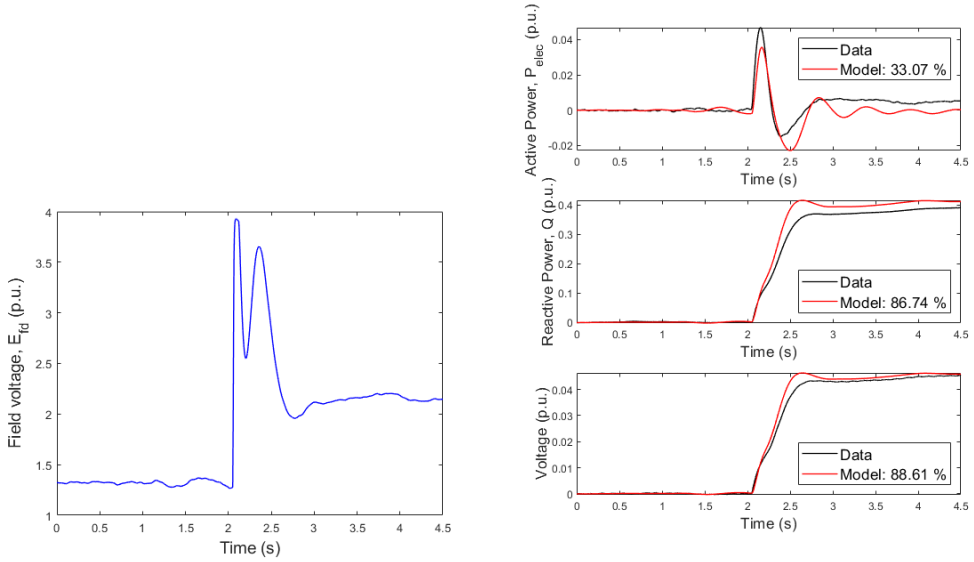

(a) Inputs to generator for validation using incorrect inputs/outputs.

(b) Generator output response comparison for incorrect inputs/outputs.

Figure C.21: Generator validation results for when X_d is increased by 10%.

References

[1] M. Marence, D. Milićević, and S. Vučina, "Hydro-power plant mostarsko blato – a multi-purpose project in karst," in *2003 Hydro*, 01 2003.

[2] M. Podlaski, L. Vanfretti, M. de Castro Fernandes, and J. Pesente, "Parameter Estimation of User-Defined Control System Models for Itaipú

Power Plant using Modelica and OpenIPSL," *2020 American Modelica Conference*, 2020.

[3] M. Podlaski, L. Vanfretti, J. Pesente and P. H. Galassi, "Automated Parameter Identification and Calibration for the Itaipú Power Generation System using Modelica, FMI, and RaPId," *7th Workshop on Modeling and Simulation of Cyber-Physical Energy Systems (MSCPES)*, pp. 1–6, 2019.

[4] J. Chow, M. Glinkowski, R. Murphy, T. Cease, and N. Kosaka, "Generator and exciter parameter estimation of fort patrick henry hydro unit 1," *IEEE Transactions on Energy Conversion*, vol. 14, no. 4, pp. 923–929, 1999.

[5] P. Pourbeik, C. Pink, and R. Bisbee, "Power plant model validation for achieving reliability standard requirements based on recorded on-line disturbance data," in *2011 IEEE/PES Power Systems Conference and Exposition*, 2011, pp. 1–9.

[6] J. Chen, P. Shrestha, S. Huang, N. D. R. Sarma, J. Adams, D. Obadina, and J. Ballance, "Use of Synchronized phasor measurements for dynamic stability monitoring and model validation in ERCOT," in *2012 IEEE Power and Energy Society General Meeting*, July 2012, pp. 1–7.

[7] H. Weber and F. Prillwitz, "Simulation models of the hydro power plants in macedonia and yugoslavia," in *2003 IEEE Bologna Power Tech Conference Proceedings,*, vol. 3, 2003, pp. 8 pp. Vol.3–.

[8] L. Ozkan, X. Bombois, J. Ludlage, C. Rojas, H. Hjalmarsson, P. Modén, M. Lundh, T. Backx, and P. Van den Hof, "Advanced autonomous model-based operation of industrial process systems (autoprofit): Technological developments and future perspectives," *Annual Reviews in Control*, vol. 42, 11 2016.

[9] K. Schroeder, J. Moyne, and D. M. Tilbury, "A factory health monitor: System identification, process monitoring, and control," in *2008 IEEE International Conference on Automation Science and Engineering*, 2008, pp. 16–22.

[10] M. A. M. Ariff, B. C. Pal, and A. K. Singh, "Estimating Dynamic Model Parameters for Adaptive Protection and Control in Power System," *IEEE Transactions on Power Systems*, vol. 30, no. 2, pp. 829–839, 2015.

[11] G. Valverde, E. Kyriakides, G. T. Heydt, and V. Terzija, "Nonlinear Estimation of Synchronous Machine Parameters Using Operating Data," *IEEE Transactions on Energy Conversion*, vol. 26, no. 3, pp. 831–839, 2011.

[12] A. Rouhani and A. Abur, "Constrained Iterated Unscented Kalman Filter for Dynamic State and Parameter Estimation," *IEEE Transactions on Power Systems*, vol. 33, no. 3, pp. 2404–2414, 2018.

[13] R. Huang, R. Diao, Y. Li, J. Sanchez-Gasca, Z. Huang, B. Thomas, P. Etingov, S. Kincic, S. Wang, R. Fan, G. Matthews, D. Kosterev, S. Yang, and J. Zhao, "Calibrating Parameters of Power System Stability Models Using Advanced Ensemble Kalman Filter," *IEEE Transactions on Power Systems*, vol. 33, no. 3, pp. 2895–2905, 2018.

[14] IEEE, "IEEE Recommended Practice for Excitation System Models for Power System Stability Studies," http://home.engineering.iastate.edu/ jdm/ee554/IEEEstd421.5-2016RecPracExSysModsPwrSysStabStudies.pdf, Dec. 2020.

[15] P. Kundur, "Power system stability," *Power system stability and control*, pp. 7–1, 2007.

[16] NEPLAN AG, "POWER SYSTEM STABILIZER MODELS: Standard Dynamic Power System Stabilizers in NEPLAN Power System Analysis Tool," NEPLAN AG, Tech. Rep., 2015. [Online]. Available: https://www.neplan.ch/wp-content/uploads/2015/08/Nep_PSSs.pdf

[17] J. Culberg, M. Negnevitsky, and K. M. Muttaqi, "Hydro-turbine governor control: theory, techniques and limitations," 2006.

[18] L. Vanfretti, M. Baudette, A. Amazouz, T. Bogodorova, T. Rabuzin, J. Lavenius, F. Jose Gomez-Lopez, "RaPId: A modular and extensible toolbox for parameter estimation of Modelica and FMI compliant models," *SoftwareX*, 2016.

[19] S. H. Jakobsen, X. Bombois, and K. Uhlen, "Non-intrusive identification of hydro power plants' dynamics using control system measurements," *International Journal of Electrical Power & Energy Systems*, vol. 122, p. 106180, 2020.

[20] M. Podlaski, L. Vanfretti, T. Bogodorova, T. Rabuzin, and M. Baudette, "Rapid-a parameter estimation toolbox for modelica/fmi-based models exploiting global optimization methods," *IFAC-PapersOnLine*, vol. 54, no. 7, pp. 391–396, 2021.

[21] J. Weber, "Description of Machine Models GENROU, GENSAL, GENTPF and GENTPJ," *PowerWorld Corporation*, 2015.

[22] NEPLAN AG, "EXCITER MODELS: Standard Dynamic Excitation Systems in NEPLAN Power System Analysis Tool," NEPLAN AG, Tech. Rep., 2015. [Online]. Available: https://www.neplan.ch/wp-content/uploads/2015/08/Nep_EXCITERS1.pdf

[23] IEEE, "IEEE Guide for Synchronous Generator Modeling Practices and Parameter Verification with Applications in Power System Stability Analyses," *IEEE Std 1110-2019 (Revision of IEEE Std 1110-2002)*, pp. 1–92, 2020.